

Research
Report

Self-acting Air-lubricated Bearing without Oil Lubrication

Masayoshi Otsuka

動圧型空気軸受

大塚正義

Abstract

One of the advanced technologies incorporated into a micro gas turbine (MGT) is the dynamic air-lubricated (no oil lubrication) bearing. We investigated the performance characteristics of a self-acting air-lubricated bearing in a 50-kWe MGT. From the results of our experiments, we were able to clarify the following.

(1) The thrust load of 300 N incurred by a 50-kWe MGT cannot be supported by the dynamic air pressure generated by a pocket-type bearing with a micro-meter size groove.

(2) The target performance (a film thickness of at least 20 μm at a load of 300 N) can be achieved by introducing compressed air (air pressure of equal to or more than 120 kPa) into the rotor disc surface through a pocket-groove.

(3) The performance characteristics of the self-acting air-lubricated bearing were improved when a new structure featuring a rear-mounted thrust bearing with a sheet-spring was adopted.

Keywords

Air bearing, Thrust load, Film thickness, Performance evaluation, Micro gas turbine, Cogeneration

要 旨

マイクロガスタービン (MGT) の先進的な技術として、オイルレスの動圧型空気軸受がある。そこで、我々は50kW級MGTを対象に動圧型空気軸受の特性を検討した。その結果、スラスト軸受について以下のことがわかった。(1) ポケット溝により発生する空気動圧のみでは荷重300Nを支持

できない。(2) 空気導入 (入口圧120kPa以上) により、目標性能 (荷重300Nで軸受すきま20 μm 以上) をクリアできる。(3) スラスト軸受面を板ばねで支持する構造を採用することで、空気軸受の特性が改善した。

キーワード

空気軸受, スラスト力, 軸受すきま, 性能評価, マイクロガスタービン, コージェネレーション

1. Introduction

For a micro gas turbine (MGT), switching from conventional oil-lubricated bearings to self-acting air-lubricated bearings (hereafter, "air bearings"), offers the following advantages.

- (1) Thermal efficiency is improved because the use of the air bearing reduces the friction loss incurred by a high-speed rotating shaft.
- (2) The size and initial cost of the MGT are reduced because an oil supply device is unnecessary.
- (3) Maintenance costs are also reduced because there is no oil and no oil supply device.

When an air bearing is adopted for the shaft of an MGT, the specifications should be considered as follows.

- (1) The shaft of the MGT rotates extremely quickly, at up to 80,000 rpm.
- (2) In an MGT, the thrust load is greater than the radial load.
- (3) Shaft vibration occurs in the event of any shaft imbalance.
- (4) Air friction can lead to large rises in the temperature.

If an air bearing is to be applied to an MGT, however, the following characteristics of the bearing must be improved.

- (1) Low stiffness and low load capacity.
- (2) Frequent occurrence of unstable oscillation.
- (3) Contact between the bearing and the shaft at start-up and stop.

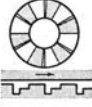


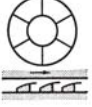
In this study, we investigated the characteristics of a thrust air bearing.

There are several kinds of thrust air bearing, as listed in **Table 1**. The 28-kWe MGT commercialized by Capstone Engineering in the later half of the 1990s uses a laminated foil bearing, like that shown in **Fig. 1**. Also, an MGT that uses an air bearing with a

bump-type foil, as shown in **Fig. 2**, was reported by Honda at the 2003 ASME conference.³⁾ The application of foil bearings to an MGT has become a new mainstream technology.

Unfortunately, the complex configuration of foil bearings may make them too expensive for commercialization. Also, foils cannot support high loads as they are easily deformed. Therefore, we decided to examine the formation of a pocket-groove on a rigid, broad bearing surface that would not deform. The appearance of the pocket-groove type bearing is shown in **Fig. 3**, and a schematic of the principle by which dynamic air pressure is generated is shown in **Fig. 4**. We know that the air flow in the circumferential direction, as induced by the interaction with the air viscosity and the rotating surface, is compressed into the groove, such that the pressure on the surface increases. This air pressure can support the thrust load that is caused by the pressure difference between the compressor and

Table 1 Types of thrust bearings.¹⁾

Classification	Step	Grooved	Pivoted	Compliant
Typical name	Step bearing	Spiral grooved	Tilting pad	Foil
Typical shape				
Characteristic	Structure is simple. Processing is easy. Stability is high. Load-index is low.	Structure is simple. Processing is easy. Stability is low, to be few load-index is high.	Structure is complex. Load-index is high. Precision is easy, to be few.	Structure is complex. Precision is easy, to be few.

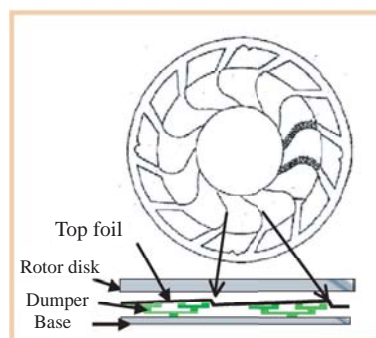


Fig. 1 Foil bearing.

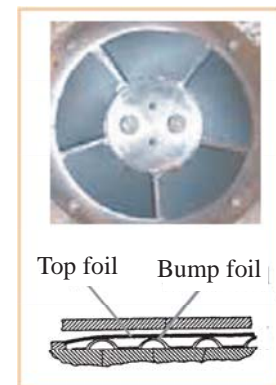


Fig. 2 Bump type foil bearing.

turbine of the MGT.

It is necessary to prevent the leakage from the periphery of the surface as this causes the air pressure to decrease. This leakage is caused by air flowing in the radial direction, as a result of the centrifugal force. A pocket shape is effective for preventing this air leakage. **Figure 5** shows a comparison of a pocket-groove-W type, a pocket-groove-N type, a step-land type, and a taper-land type and indicates that the pocket-groove type offers the best performance characteristics for a given film thickness.

2. Target air bearing performance for an MGT

2.1 Estimation of thrust load and film thickness

To estimate the thrust load, we assumed the use of a 50-kWe class MGT. As shown in **Fig. 6**, the thrust load increases in proportion to the rotor speed, but the film thickness decreases.

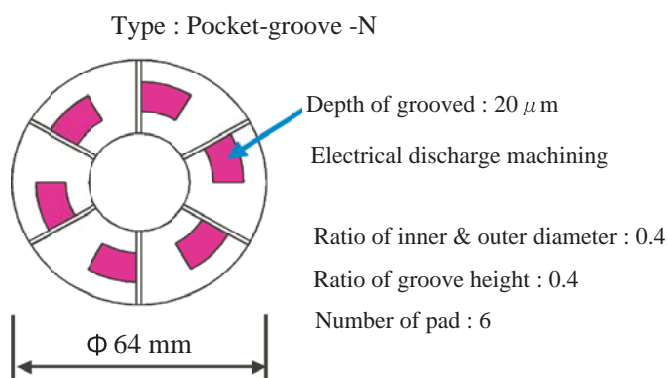


Fig. 3 The shape and the specification of the pocket-groove type bearing.

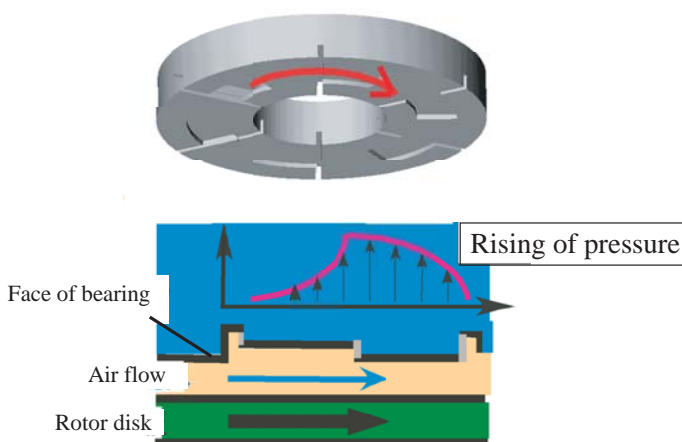


Fig. 4 The principle of the groove-type dynamic air pressure bearing.

speed of 80,000 rpm, the thrust load is estimated to be about 260 N. It is assumed that a film thickness equal to or greater than $22 \mu\text{m}$ is needed to support this thrust load.

In the early stages of our investigation, we aimed temporarily at a target film thickness equal to or greater than $20 \mu\text{m}$ for a thrust load of 300 N at a rotor speed of 80,000 rpm.

2.2 Bearing characteristics

We calculated a bearing outer diameter that satisfies the target value by using a relational expression for the bearing characteristics.

The following expression links the bearing number

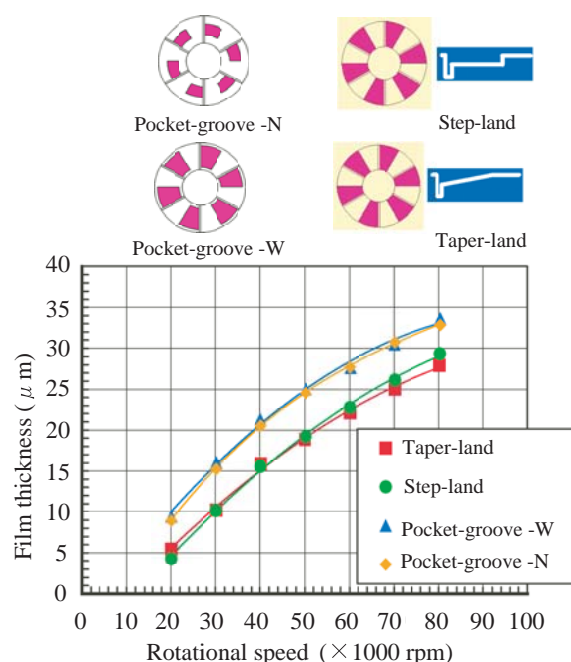


Fig. 5 The comparison between a pocket-groove type and a step type.

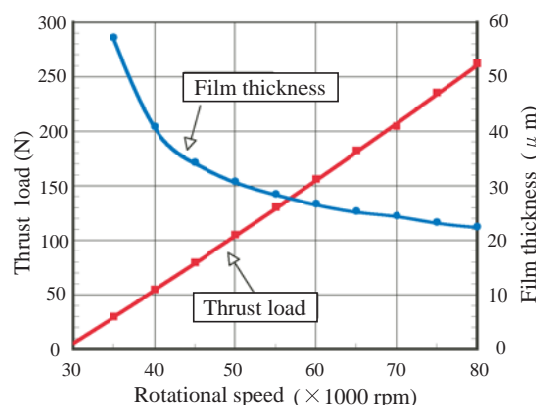


Fig. 6 The estimation of thrust load.

and the dimensionless load carrying capacity.

The bearing Number Λ_c is defined by Eq. (1)

$$\Lambda_c = \frac{3 \cdot \mu \cdot \omega \cdot (R_o^2 - R_i^2)}{P_a \cdot h^2} \dots \dots \dots (1)$$

μ : Viscosity

ω : Angular velocity

P_a : Ambient pressure

h : Film thickness

The dimensionless load carrying capacity W_n is defined by Eq. (2)

$$W_n = \frac{W}{\pi \cdot P_a \cdot (R_o^2 - R_i^2)} \dots \dots \dots (2)$$

W : Load

R_o : Bearing outer radius

R_i : Bearing inner radius

π : Circular constant

Figure 7 shows the relationship between the bearing number and the dimensionless load carrying capacity. **Figure 8** shows the relationship between the bearing outer diameter and the load when the film thickness is held constant at 20 μm with a ratio of 0.4 between the outer and the inner diameter. From Fig. 8, we find that an outer diameter equal to or more than 100 mm is needed in order to support loads of 300 N at a rotor speed of 80,000 rpm.

3. Investigation of design of self-acting air-lubricated bearing

We studied the thrust air bearings in two stages.

(1) In the first stage, we evaluated the performance

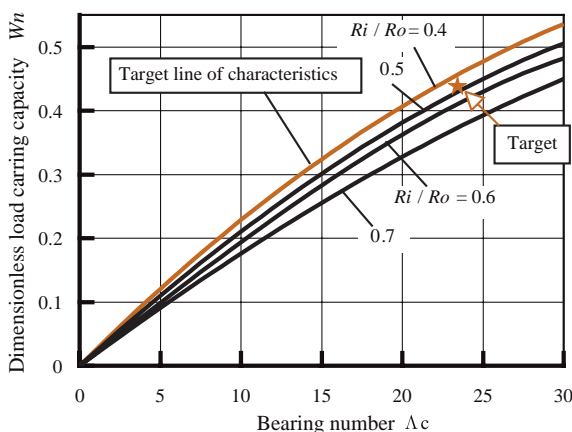


Fig. 7 Characteristics of spiral grooved air bearings.

characteristics of the air bearing at rotational speeds up to 80,000 rpm. We chose to do this because there were no reports on the performance of air bearings at ultra high-speed rotational speeds.

(2) In the second stage, we demonstrated the thrust load of 300 N at a rotational speed of 80,000 rpm because, again, there were no reports in the literature.

3.1 Basic test at high rotational speed

3.1.1 Test rig and experimental method

We developed a basic test rig for evaluating the bearing characteristics. A schematic of this test rig is shown in **Figs. 9**. A photograph of the rig is shown in **Fig. 10**. The test rig consists of a rotor disk, a drive unit, a bearing attachment, bearing supports, a load and associated measurement instruments, and an air-damped mount.

The features of the test rig are as follows:

1) The rotational shaft is oriented horizontally even though it is vertical in practical applications.

2) A bearing surface is configured on the stationary side even though it is on the rotating side in practical applications. With this configuration, the surface of the circular disc can support the load uniformly, and the load can be adjusted easily. This configuration also makes it easy to measure the film thickness, the friction torque, and so.

The specifications of the test rig are as follows.

- (1) The rotor speed is set to between 5,000 rpm and 100,000 rpm (varied continuously)
- (2) The load is increased from 15 N to 55 N (in 0.5-N increments)
- (3) The bearing outer diameter is 64 mm or 68 mm (to a maximum of 100 mm)

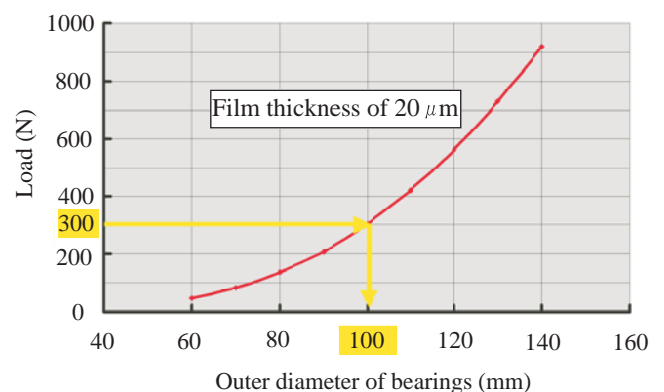


Fig. 8 The estimation of the bearing outer diameter.

The measured terms (which are mainly the static characteristics) are as follows.

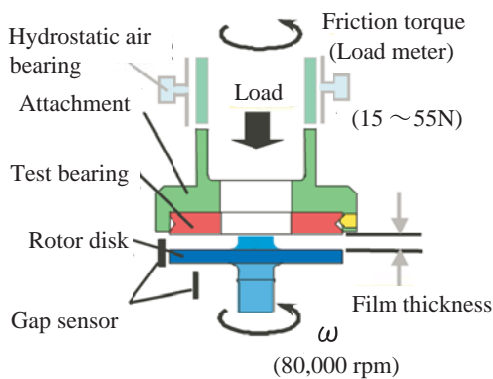
- (1) The film thickness is defined as the bearing clearance, as measured by an eddy current type gap sensor.

Film thickness = displacement of the bearing - displacement of the rotor disk

- (2) Friction torque is calculated by measuring with a load meter.

Friction torque = load * radius (measured position)

A bearing armature is lowered to a point near the rotor surface once the desired rotor speed has been reached. Then, we confirm that the bearing

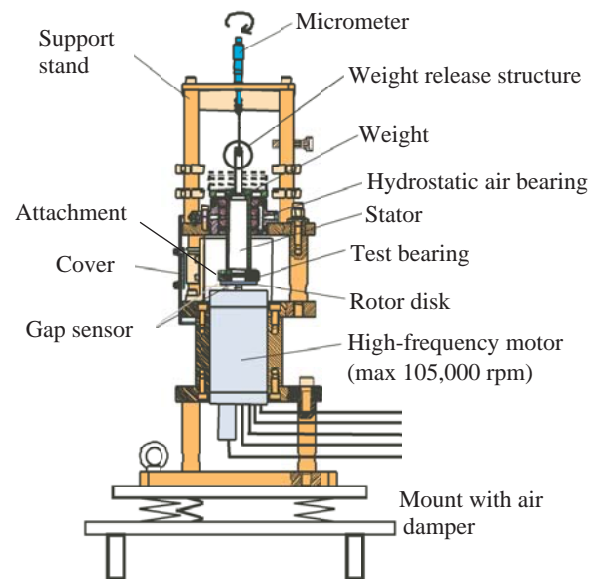


(a) Enlargement on the measuring part.

armature is not touching the rotor surface and that it is stable. Once the bearing system is stable, the displacement between the bearing and the rotor disk, and the load incurred by the viscous friction of the air and the temperature, are measured. The film thickness is calculated from the displacement, while the friction torque is calculated from the load.

3.1.2 Test results

The specifications of the test bearings are listed in **Table 2**. The film thickness and the friction torque



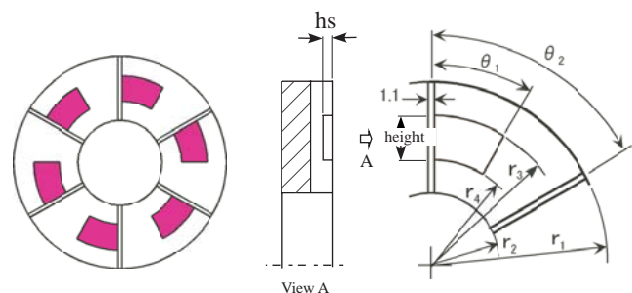
(b) Basic test rig.

Fig. 9 Schematic of the basic test rig.

Table 2 Specification of a thrust air bearing.



Fig. 10 Photograph of the basic test rig.



Outer diameter	r_1	64 mm
Ratio of outer to inner diameter	r_2/r_1	0.4
Groove angle	θ_1	30 °
Pad angle	θ_2	60 °
Ratio of groove height	$P_p (= (r_3 - r_4) / (r_1 - r_2))$	0.4 μm
Groove depth	h_s	20
Total number of pad	P_n	6
Field coarseness		1.6 z

of the pocket-groove type bearing are shown in **Figs. 11**. Figure 11(a) shows the obtained performance characteristics for a rotor speed from 20,000 rpm to 80,000 rpm at a bearing load of 15 N. Figure 11(b) shows the performance characteristics for loads between 15 N and 35 N at a rotational speed of 80,000 rpm. The film thickness is almost proportional to the rotor speed and is inversely proportional to the load. The friction torque is proportional to both the rotor speed and the load. Although the film thickness is almost proportional to the rotor speed up to 40,000 rpm, the film thickness at rotor speeds in excess of 40,000 rpm increases at a low rate. The friction torque is directly proportional to the rotor speed. The surface temperature of the bearings rises by about 20 °C between 20,000 and 80,000 rpm, which constitutes a considerable differential.

Our preliminary investigation revealed the measured characteristics to be inferior to the estimated target characteristic line, as shown in **Fig. 12**. Therefore, the performance characteristics of the trial air bearings must be improved to reach the target.

3.2 Factors leading to non-achievement of target performance and measures

In this chapter, we consider the reasons for the film thickness being smaller than the target value.

3.2.1 Degradation factors

(1) Insufficient increase in dynamic air pressure

The dynamic pressure that is generated in the pocket-groove is relatively small, compared to the initial estimate.

(2) Decrease in the generated dynamic air pressure

The generated dynamic air pressure fell for several reasons, as follows.

(i) Misalignment and deformation of the rotor disk and the bearing

The rotor disc of the thrust bearing and the bearing's surface with the groove are completely parallel in the ideal design. However, there is deformation of the rotor disk caused by geometric differences, centrifugal force, and the load. There is also an inclination of several microns to 10 μm caused by inaccuracies in the forming accuracy and in the perpendicularity of the axis, and so on. Because this inclination causes a crack in the non-

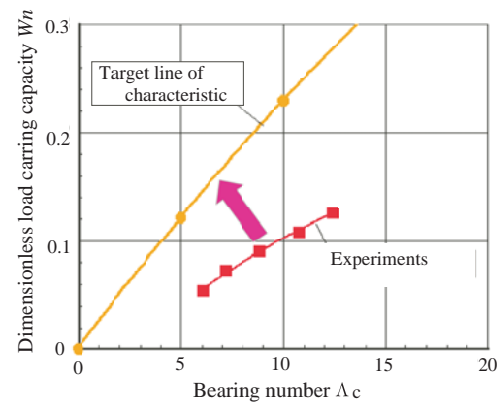


Fig. 12 Difference of the bearing characteristic between experiments and target line.

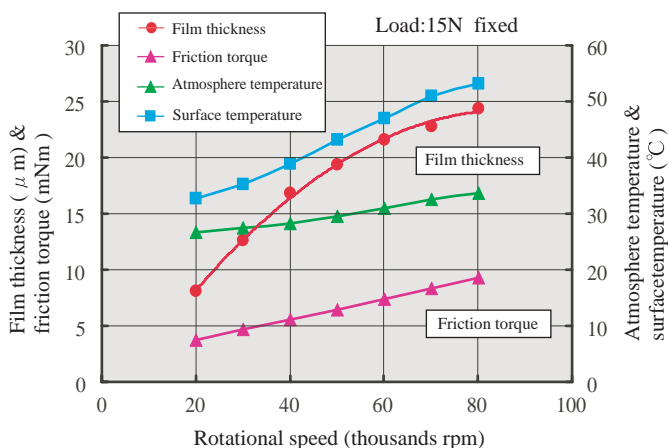


Fig. 11(a) Characteristics with rotor speed.

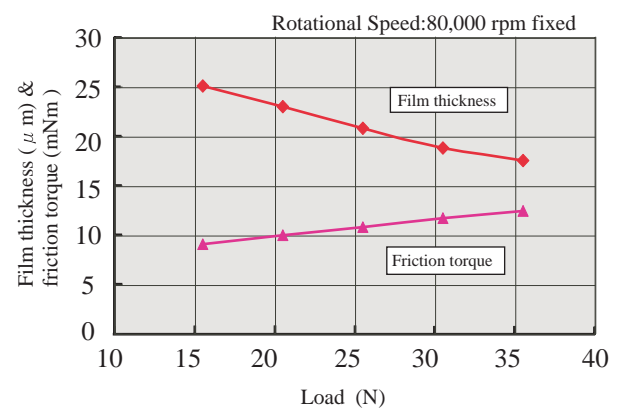


Fig. 11(b) Characteristics with load.

parallel gap, the increased air pressure falls relative to that on the side of the larger crack (**Fig. 13(a)**). Also, because the rotational speed of 80,000 rpm is very high and the centrifugal force extends the rotor disc surface in the radial direction, distortion of the circular disc surface occurs and the flatness of the surface is lost (**Fig. 13(b)**).

The values calculated by a FEM analysis are shown in **Fig. 14**. This calculation indicates that part of the rotor disk tip is bent as a result of the generated pressure.

(ii) Centrifugal whirling of the rotor disk caused by eccentricity of the rotational axis

Centrifugal whirling occurs when there is a difference in the straightness of the rotor axis. Because of the misalignment and the deformation of the disk and bearing surfaces, the dynamic air pressure decreases (**Fig. 13(c)**).

3. 2. 2 Improvements

The following improvements were reviewed as a means of overcoming those factors that lead to degradation.

(1) Optimization of the groove shape

The bearing characteristics are influenced by the shape of the bearing surface. The results of our examining the groove depth and the groove height are shown in **Figs. 15(a)** and **(b)** (also see Table 2). These results indicate that the bearing characteristics can be improved by making the groove deeper and expanding it in the radial direction. **Figure 15(c)** shows that the bearing characteristics approach the target line as a result of changing the bearing groove shape.

(2) Air introduction

It is possible to improve the bearing characteristics when the static pressure rises, based on the estimation using the bearing characteristic equations. We confirmed that the film thickness expanded as a result of introducing compressed air into the rotor disc surface from the centre of the test rig. **Figure 16** shows the groove bearing characteristic improvements obtained by introducing the compressed air. The film thickness expands as a result of increasing the air pressure.

(3) Shape and surface roughness of the rotor disk

We created a convex area in the centre of the rotor on the bearing surface, and improved the surface processing precision. As a result of this, we should aim to reduce the flexing caused by the centrifugal force and the surface friction.

(4) Provision of sheet-spring structure support

We employed a structure supported with a sheet-spring to follow the movement of the armature. A variety of spring-based structures have been proposed in patents, but we contrived the structure described below. A lamina disk with a thickness of 0.1 to 0.3 mm and a surface groove is positioned behind the bearings, the perimeter of the disk is fixed to the bearing, and the internal circumference of the disk is fixed to the bearing base. A bearing with this structure can decline even if the pressure load is partially taken by the perimeter of the disk. A test result is shown in **Fig. 17**. The film thickness

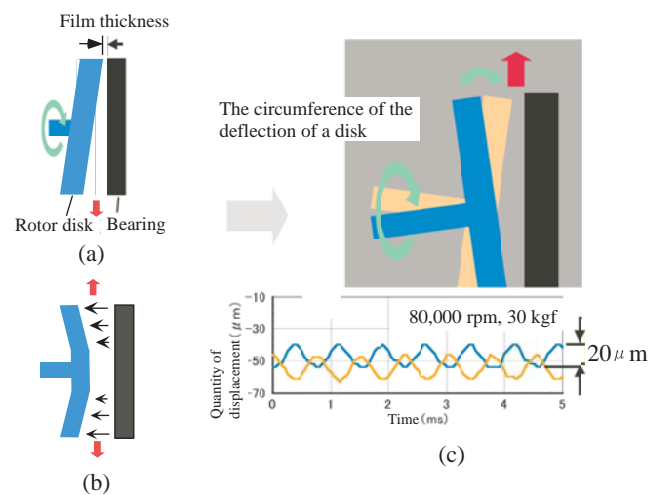


Fig. 13 Dynamic behavior of the rotor disk and the bearing.

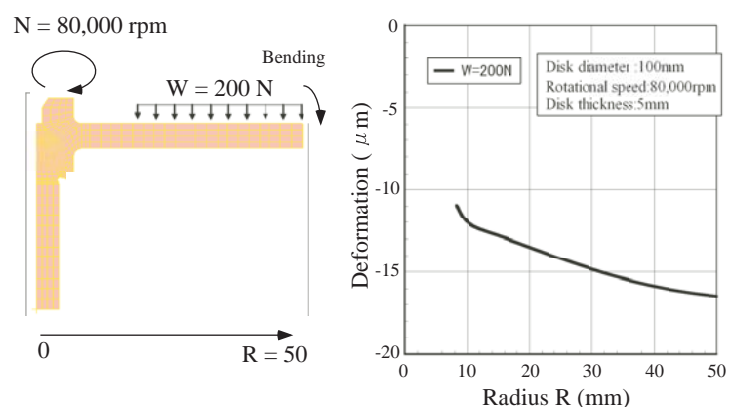


Fig. 14 Deformation of the rotor disk calculated by a FEM analysis.

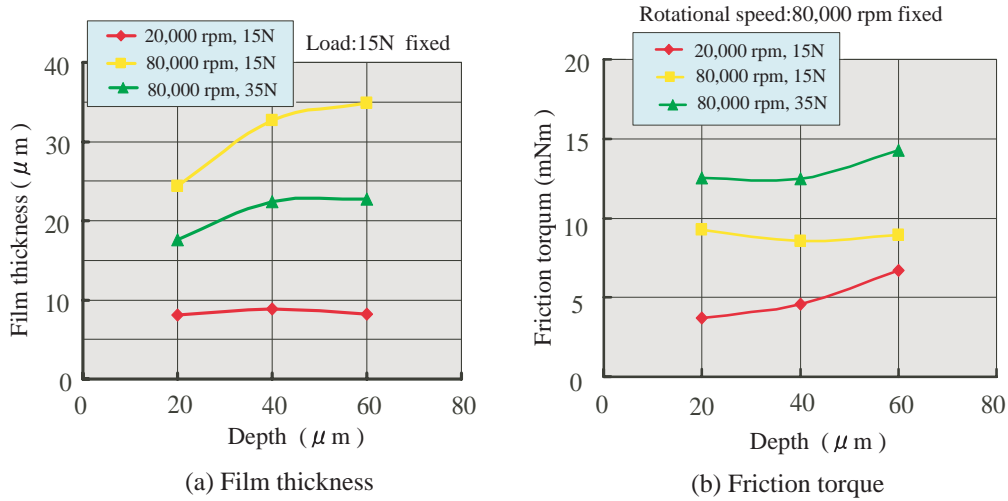


Fig. 15(a) Influence of the groove depth.

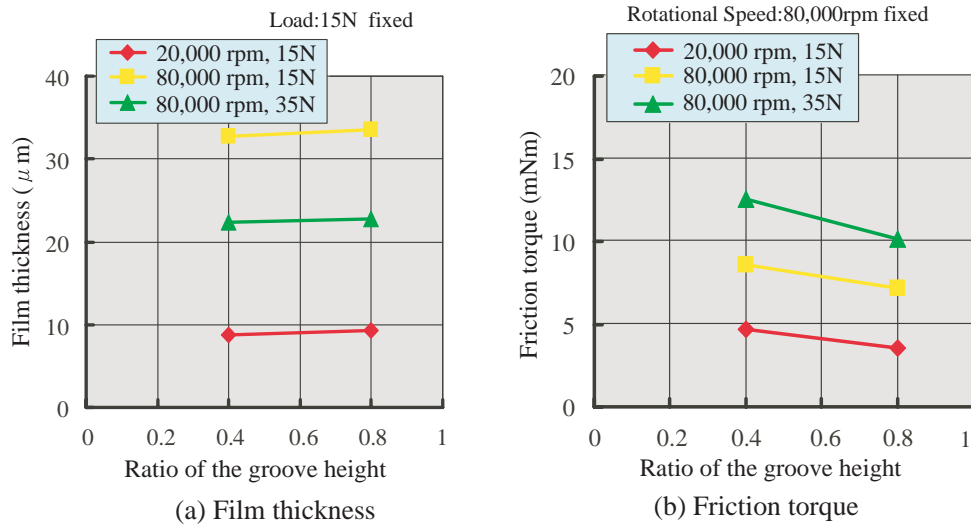


Fig. 15(b) Influence of the groove height.

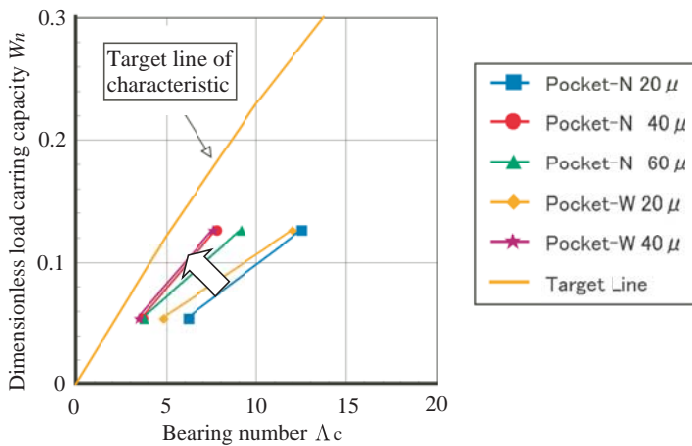


Fig. 15(c) Bearing characteristics.

becomes large as a result of employing the sheet-spring structure, so we can conclude that this structure is very effective.

4. Proof test

4.1 High-speed and high-load test

The purpose of this test was to achieve the target value (rotor speed of 80,000 rpm, load of 300 N, film thickness in excess of 20 μm) while reducing the bearing outer diameter. When incorporating a thrust bearing into an actual MGT, it is important that the bearing outer diameter be made as small as possible, because an outer diameter of 100 mm is too large for the 50-kWe class MGT.

4. 1. 1 Test rig

Our high-load test rig is shown in **Fig. 18**. The rotational shaft of the test rig is oriented horizontally, unlike the basic test rig in which the shaft is oriented vertically. The structure of the bearings is basically same as in the basic test rig, but differs in that the load is supported by a coil spring and the rotor is driven by a turbine.

4. 1. 2 Test results

As the load was increased, the rotor disk would tend to contact the bearings more easily because the film thickness decreases as the load increases. Therefore, the test was carried out after setting the rotor speed to 80,000 rpm and increasing the film thickness by introducing compressed air from the start of the test. The results obtained for a bearing outer diameter of 100 mm are shown in **Fig. 19**. The film thickness remained relatively constant at about 70 μm for loads of 50 N to 250 N, because the inlet air pressure was increased from 30 kPa to 100 kPa. After that, the air pressure was held at 100 kPa and the load was increased from 250 N to 300 N. Then, the film thickness decreased, but the film thickness of 55 μm at 300 N surpassed the target value of at least 20 μm . The ambient temperature increased by 120 $^{\circ}\text{C}$ because the load of 300 N had an exothermic effect.

Figure 20 shows the results of examining the effect of varying the supplied air pressure for bearing outer diameters of 100 mm and 80 mm. The film thickness fell to

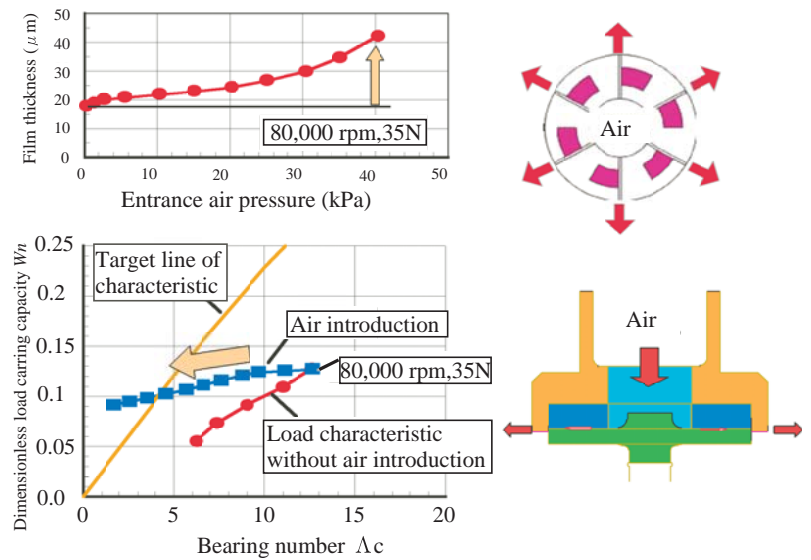


Fig. 16 Characteristics of the groove bearing improved by the air introduction.

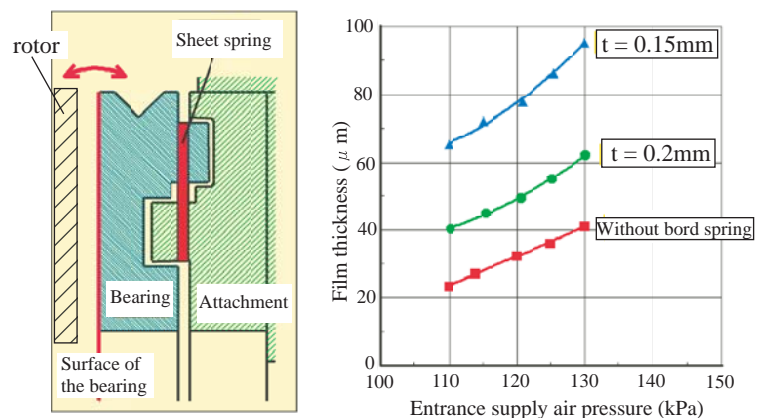


Fig. 17 Examination of spring structure. Film thickness increased by air introduction and the effect of the structure of the bearing with a sheet spring.

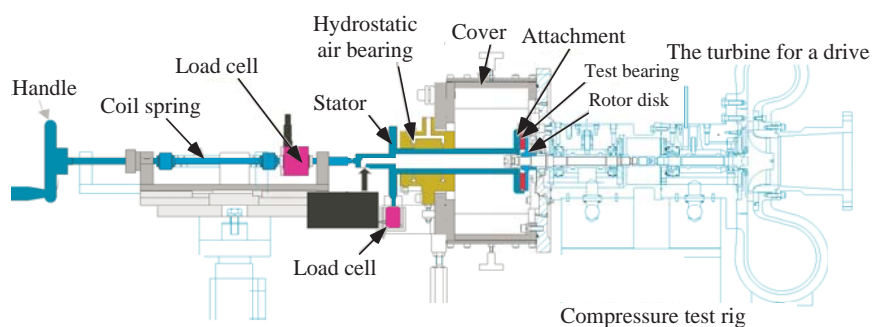


Fig. 18 Test rig for high-load experiment.

30 μm when the air pressure was dropped to 80 kPa for a bearing outer diameter of 100 mm. Because the performance declines in case of a bearing outer diameter of 80 mm, the inlet air pressure must be increased in order to achieve the same film thickness as that obtained for a diameter of 100 mm. The figure shows that the target of a film thickness of at least 20 μm can be secured when the air pressure is maintained at least 120 kPa. In other words, we can say that an air bearing for an MGT cannot be realized successfully without introducing air. Actually, an MGT can use air from its compressor. Introducing compressed air from the impeller exit would allow us to attain the goal needed for an MGT. Because the target MGT has an impeller delivery pressure of about 150 kPa, we could realize an air bearing with an outer diameter of 80 mm.

4. 2 Proof test in an actual rotor

We incorporated the developed thrust air bearings into a compressor test rig which closely approximated the shape of an actual rotor, and then evaluated the performance characteristics.

We investigated the following items.

- (1) Handling of rotor resonance caused by imbalance, particularly at start-up and stop
- (2) Effect of the performance

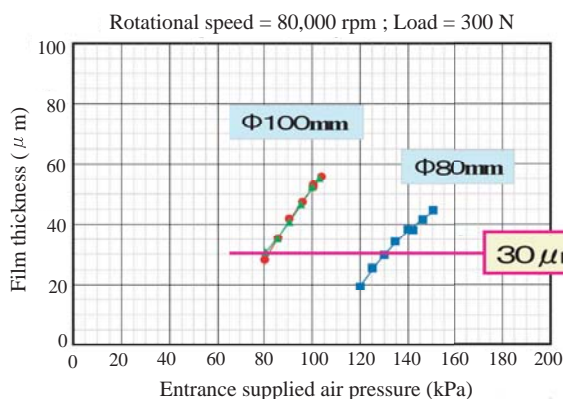


Fig. 20 The difference of the film thickness between 80mm and 100mm of the bearing outer diameter.

improvement attained through impeller delivery pressure introduction

Regarding the resonance caused by imbalance of the rotor assembly, our computational analysis indicated that the 1st and the 2nd rotational modes exist in the low-speed range of around 6,000 rpm and 20,000 rpm, as shown in **Fig. 21**. These resonance points of the rotor dynamics must be overcome. The resonant frequency of the rotor assembly is not a problem because a bending mode of the rotor exists at rotational speeds equal to or greater than 85,000 rpm, which is in excess of the

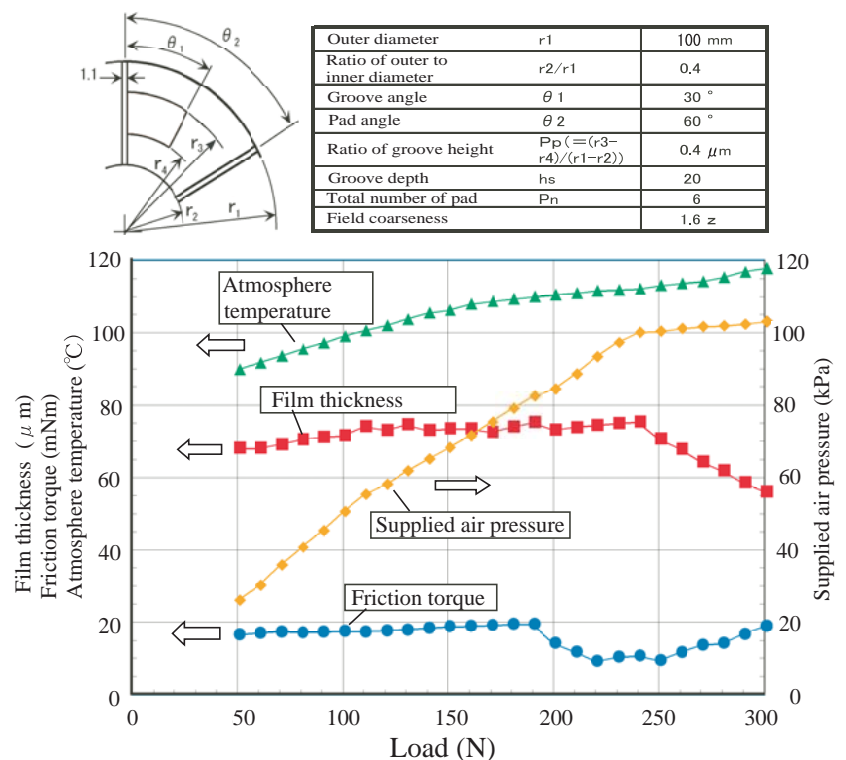


Fig. 19 Experimental result.

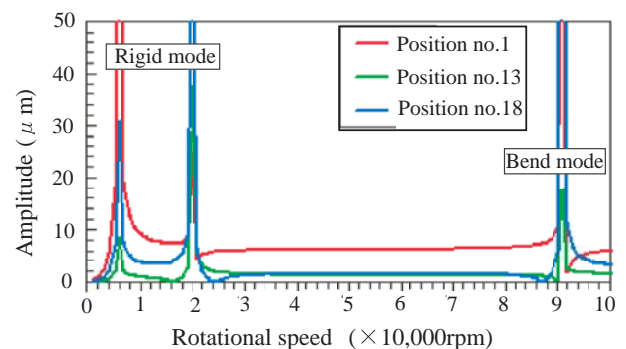


Fig. 21 Resonant frequency of the shaft assembly.

rated speed of the target MGT.

To cope with the contact between the bearings and the rotor disk at start-up and stop, some finishes for the bearing surface were reviewed and, as a result, we selected the following finish.

Bearing surface: The material was heat-treated (quenching, tempering) and the strip surface roughness was minimized in the manufacturing process.

Armature surface: The surface was coated with solid MoS_2 lubricant.

4. 2. 1 Groove shape on bearing surface

Considering the actual size of the MGT, we decided to employ an outside bearing diameter of 80 mm, and the bearing surface groove shape shown in **Fig. 22**. Given our previous results, the groove shape of the pocket type bearing surface was designed as shown in the figure and the groove was kept shallow at the outer circumference.

4. 2. 2 Assembly test rig

A schematic of our assembly test rig is shown in **Fig. 23**. The test rig was remodeled from one used for a centrifugal compressor which employed ball bearings. The bearing part of the test rig is such that the thrust load is carried by the air bearing but the radial load is carried by an oil-lubricated roller bearing. In the first part of this test, the operation of the air bearings was confirmed when sufficient compressed air was supplied. In the next step, we confirmed that sufficient compressed air could be delivered from the impeller exit.

4. 2. 3 Results

The results of introducing air from the impeller exit are shown in **Fig. 24**. These results indicate a time span

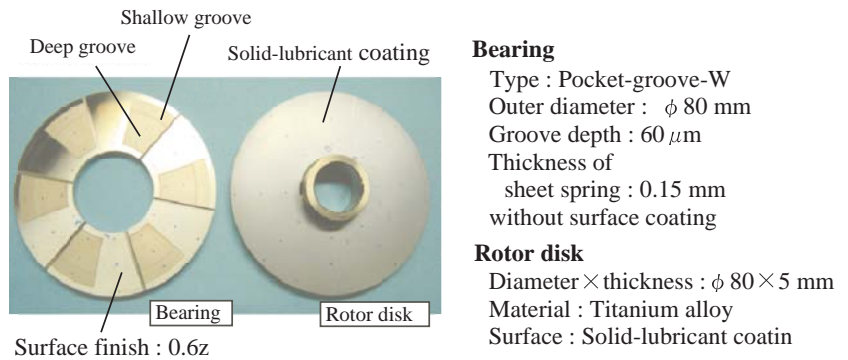


Fig. 22 The shape of the air bearing.

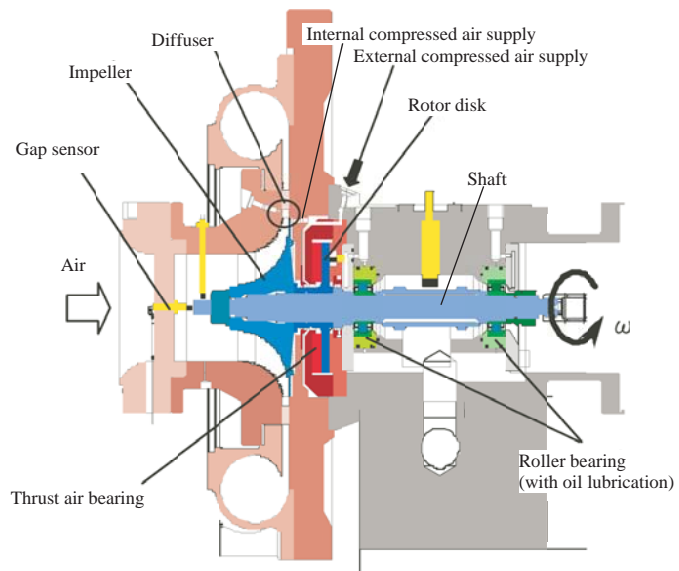


Fig. 23 Schematic of the assembly test rig.

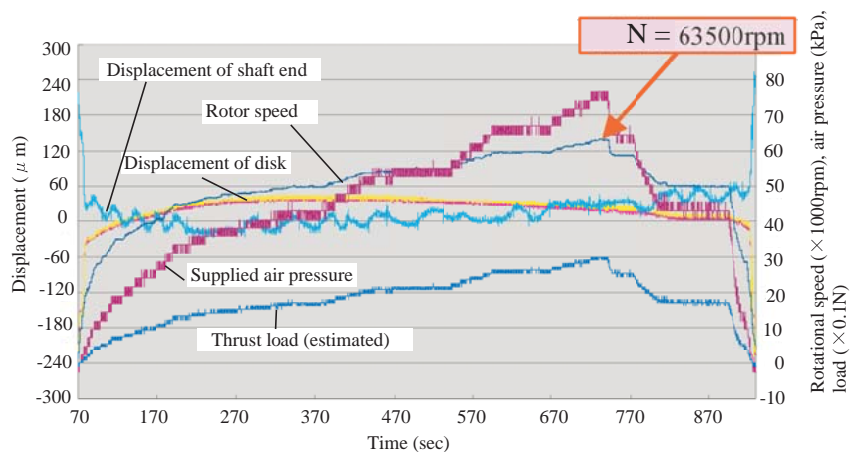


Fig. 24 Experimental result (1).

from start-up to the point where a rotational speed of 60,000 rpm is reached. We were able to confirm stable operation of the air bearings. The impeller delivery pressure increased depending on the increase in the rotor speed, while the displacement of the rotor disk fell. The pressure delivered by the impeller was 80 kPa at 60,000 rpm, while we estimated a thrust load of 300 N. The impeller-delivered pressure was lower because the rotor speed was lower than that of the high-load test, but the thrust load was comparatively high. The thrust load actually improved slightly compared with the value which was calculated from the impeller-delivered pressure.

Also, no problems were observed in continuous operation equal to or more than 15 minutes at 50,000 rpm, as shown in Fig. 25.

5. Summary

A dynamic air pressure bearing without oil lubrication is an important core technology for a micro gas turbine (MGT). We investigated the performance characteristics of a self-acting air-lubricated bearing for a 50-kWe class MGT. As an air bearing for the MGT, we investigated the effect of different groove types on dynamic air pressure bearings. Our investigation of the thrust bearing clarified the following points.

(1) In the early stages of our investigation, we aimed at a target film thickness of at least 20 μm for a thrust load of 300 N and a rotor speed of 80,000 rpm.

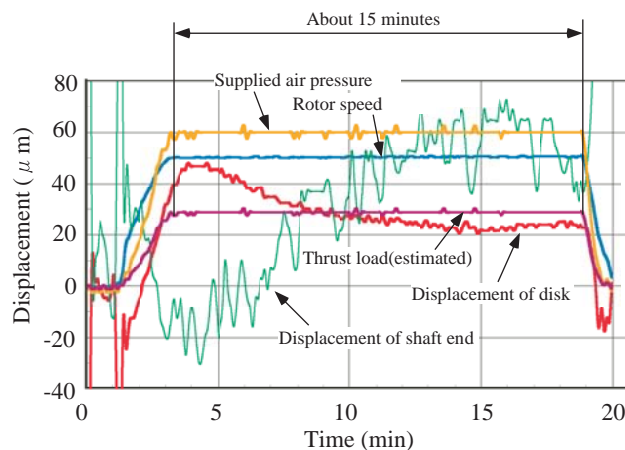


Fig. 25 Experimental result (2).

(2) Pocket-type groove shapes were reviewed using a basic test rig running at speeds between 20,000 and 80,000 rpm, and we selected the best of these shapes.

(3) When employing a high-load test rig capable of applying a load of 300 N at a rotational speed of 80,000 rpm, we were able to achieve the target value (more than 20 μm) by adapting a sheet-spring structure with a disc diameter of 80 mm, less than the 100 mm of the preliminary design, and by introducing air at a pressure equal to or more than 120 kPa.

(4) The developed air bearing was evaluated at a maximum rotor speed of 60,000 rpm with an assembly test rig which imitated the actual gas generator of an MGT, and the test involving continuous running for 15 minutes at 50,000 rpm was carried out. As a result, we were able to clarify the practicality of using a pocket-groove type dynamic air pressure bearing supported by a sheet-spring.

References

- 1) Togo, S. : "Kitajikuu -Sekkei kara Seisaku made-", (in Japanese), (1999), Kyoritsu Shuppan
- 2) RPI-MTI Gas-Bearing Design Course
- 3) Microturbine Equipment Panel, ASME Turbo Expo., Atlanta, 16-19 June 2003
- 4) Shimura, K. : "Microturbine Research at Honda", ASME Pap. No.2003-GT-39055(2003)
- 5) Ochiai, M. and Hashimoto, H. : "Static and Dynamic Characteristics of High-Speed, Stepped Thrust Gas-Film Bearings", Trans. of JSME, C, (in Japanese), **64**-628(1998), 305-312
- 6) Ochiai, M. and Hashimoto, H. : "Measurements of Compressibility Effects in Stepped Thrust Gas Film Bearing", Tribol. Trans., **42**-4(1999), 723-730
- 7) Hashimoto, H., et al. : 2001 *endo Nenjitaikai Kouen Ronbunshuu*, (in Japanese), (2001), JSME
- 8) Hashimoto, H., et al. : 2002 *endo Nenjitaikai Kouen Ronbunshuu*, (in Japanese), (2002), JSME
- 9) Capstone Turbine co. Ltd. : Jpn. Transl. PCP. H09-510522, (in Japanese)

(Report received on Dec. 23, 2005)



Masayoshi Otsuka

Research fields : Gas Turbine

(Aerodynamics, CFD Analysis)

Academic society : Jpn. Soc. Mech. Eng., Gas Turbine Soc. Jpn.